

Research article

EP300 regulates the SLC16A1-AS1-AS1/TCF3 axis to promote lung cancer malignancies through the Wnt signaling pathway

Yunhao Sun^a, Jian Sun^a, Kaijun Ying^a, Jinjin Chen^b, Tingting Chen^c, Leilei Tao^b, Weigang Bian^b, Limin Qiu^{a,*}

^a Department of Thoracic Surgery, The First People's Hospital of Yancheng City, The Yancheng Clinical College of Xuzhou Medical University, Yancheng, Jiangsu, 224005, PR China

^b Oncology Department, The First People's Hospital of Yancheng City, The Yancheng Clinical College of Xuzhou Medical University, Yancheng, Jiangsu, 224005, PR China

^c Department of Emergency, The First People's Hospital of Yancheng City, The Yancheng Clinical College of Xuzhou Medical University, Yancheng, Jiangsu, 224005, PR China

ARTICLE INFO

Keywords:

EP300
SLC16A1-AS1
TCF3
Lung cancer
Wnt/ β -catenin pathway

ABSTRACT

Objective: To investigate the regulatory mechanism of EP300 in the interaction between SLC16A1-AS1 and TCF3 to activate the Wnt pathway, thereby promoting malignant progression in lung cancer.

Methods: In lung cancer cell lines, SLC16A1-AS1 was knocked down, and the impact of this knockdown on the malignant progression of lung cancer cells was assessed through clonogenic assays, Transwell assays, and apoptosis experiments. The regulatory relationship between EP300 and SLC16A1-AS1 was investigated through bioinformatic analysis and ChIP experiments. The expression of SLC16A1-AS1 and TCF3 in 56 paired lung cancer tissues was examined using RT-qPCR, and their correlation was analyzed. The interaction between TCF3 and SLC16A1-AS1 was explored through bioinformatic analysis and CoIP experiments. Activation of the Wnt/ β -catenin pathway was assessed by detecting the accumulation of β -catenin in the nucleus through Western blotting. The role of EP300 in regulating the effect of SLC16A1-AS1/TCF3-mediated Wnt/ β -catenin signaling on lung cancer malignant progression was validated through in vitro and in vivo experiments.

Results: SLC16A1-AS1 is highly expressed in lung cancer and regulates its malignant progression. EP300 mediates histone modifications on the SLC16A1-AS1 promoter, thus controlling its expression. SLC16A1-AS1 exhibits specific interactions with TCF3, and the SLC16A1-AS1/TCF3 complex activates the Wnt/ β -catenin pathway. EP300 plays a critical role in regulating the impact of SLC16A1-AS1/TCF3-mediated Wnt/ β -catenin signaling on lung cancer malignant progression.

Conclusion: EP300 regulates the SLC16A1-AS1/TCF3-mediated Wnt/ β -catenin signaling pathway, influencing the malignant progression of lung cancer.

* Corresponding author.

E-mail address: qlm2007qlm@163.com (L. Qiu).

1. Introduction

Lung cancer (LC), accounting for the second most prevalent (11.4%) cancer worldwide and the leading cause of cancer-related deaths (18%) in 2020 [1–3], continues to pose a significant global health challenge. In China, LC stands as the predominant cancer type, boasting the highest incidence and mortality rates among all cancer types [4–6]. Approximately 85% of diagnosed patients belong to the histological subtype known as non-small cell lung cancer (NSCLC), with lung adenocarcinoma (LUAD) and lung squamous cell carcinoma (LUSC) being the most prevalent subtypes [7,8]. The most effective and primary treatment for early-stage NSCLC is surgical resection, while chemotherapy or radiation therapy is reserved for patients who are no longer suitable candidates for surgery [9,10]. However, patients with advanced LC often face a grim prognosis, necessitating urgent efforts to identify potential biomarkers and develop therapeutic targets for early diagnosis and effective intervention.

In recent years, technological advances in transcriptome profiling revealed that the repertoire of human RNA molecules is more diverse and extended than originally thought. Long non-coding RNAs (lncRNAs), arbitrarily defined as over 200 nucleotides in length, have been increasingly recognized as key molecules involved in diverse pathological conditions including cancers when aberrantly expressed [11,12]. Not surprisingly, aberrant expression patterns of lncRNAs have been associated with the onset and progression of LC [13]. In this study, by conducting a lncRNA microarray analysis using three pairs of LC tissues and their matched adjacent cells, we obtained SLC16A1 antisense RNA 1 (SLC16A1-AS1) as an aberrantly highly expressed lncRNA in LC. Upregulation of SLC16A1-AS1 has been detected in LC tissues and its knockdown led to suppressed malignant phenotype of the LC cells [14,15]. However, the underpinning regulatory mechanism for its upregulation, as well as the downstream molecules involved in its oncogenic events, are largely unknown.

Interestingly, we obtained from bioinformatics prediction that there are significant binding peaks of E1A binding protein p300 (EP300) and acetylation of lysine 27 on histone 3 (H3K27ac) near the SLC16A1-AS1 promoter. H3K27ac is a well-established mark of active enhancers and genes regulated by such super-enhancers are enriched for oncogenic transcription factors [16]. EP300, also known as p300, along with CREB-binding protein (CBP), is a large multifunctional coactivator that possesses intrinsic histone acetyltransferase activity and establishes the gene expression regulated by H3K27ac [17,18]. Indeed, the EP300-mediated H3K27ac modification has been frequently found to be responsible for oncogene activation and malignant progression of cancer cells [19,20]. Based on the bioinformatics prediction and the existing evidence, we hypothesized that the aberrant SLC16A1-AS1 activation might be ascribed to the enrichments of EP300 and H3K27ac modifications at its promoter. This study was then performed to verify this hypothesis and to further explore the downstream molecules affected by SLC16A1-AS1 during LC progression.

2. Materials and methods

2.1. Clinical samples

Fifty-six pairs of LC and matched adjacent tissues were collected from LC patients treated at our hospital from May 2021 to March 22. All patients had complete clinical data, were diagnosed for the first time, and did not have other malignant tumors. The study protocol was approved by the hospital's Ethics Committee and informed consent was obtained from all patients. The clinical trials were strictly adhered to the *Declaration of Helsinki*.

2.2. Cell culture and treatment

LC cell lines (H1299 and Calu-3) were procured from Otwo Biological Technology Co., Ltd. (Shenzhen, Guangdong, China), while another two LC cells (HS 683 and T98G) and a human microglial cell line (HMC3) were procured from Procell Life Science & Technology (Wuhan, Hubei, China). All cells were maintained in Dulbecco's modified Eagle's medium (Thermo Fisher Scientific, Rockford, IL, USA) supplemented with 10% fetal bovine saline and 1% penicillin-streptomycin and cultured at 37 °C with 5% CO₂.

The lentivirus-packaged short hairpin (sh) RNAs of SLC16A1-AS1 and EP300 (sh-SLC16A1-AS1#1–3 and sh-EP300-AS1#1–3), and the gene overexpression lentivirus of SLC16A1-AS1 and TCF3 (oe-SLC16A1 and oe-TCF3) were provided by VectorBuilder Inc. (Guangzhou, Guangdong, China) and administrated into H1299 and Calu-3 cell lines. After 24 h, the cell lines were transferred into a fresh medium for another 24 h of culture. Stably infected cells were screened using puromycin.

For artificial inhibition of β -catenin, the H1299 and Calu-3 cells were treated with XAV-939 (MedChemExpress, Monmouth Junction, NJ, USA) at 1 μ M for 48 h. Cells treated with an equal volume of dimethyl sulfoxide (DMSO) solution were set to control.

Table 1
Primers for qPCR.

Symbol	Forward	Reverse
GAPDH	GTCTCCTCTGACTTCAACAGCG	ACCACCCCTGTGCTGTAGCCAA
SLC16A1-AS1	TAGGCAATCTGCCCTCGTTC	CAGGCCTCTCGGTGACTTTT
EP300	GATGACCCTTCCCAGCCTCAA	GCCAGATGATCTCATGGTGAAGG
TCF3	GATGACCCTTCCCAGCCTCAA	GCCAGATGATCTCATGGTGAAGG

2.3. Reverse transcription-quantitative polymerase chain reaction (RT-qPCR)

Total cellular RNA was extracted using the TRIzol reagent (Thermo Fisher Scientific), which was applied to real-time PCR amplification using the SuperScript™ III Platinum™ SYBR™ Green One-Step qRT-PCR Kit (Thermo Fisher Scientific) on the ABI7500 PCR system (Applied Biosystems, Inc., Carlsbad, CA, USA). All procedures were conducted in strict accordance with the manufacturer's protocol. Relative gene expression normalizing to the endogenous loading glyceraldehyde-3-phosphate dehydrogenase (GAPDH) was evaluated using the $2^{-\Delta\Delta C_t}$ method. The primer sequences are displayed in Table 1.

2.4. Colony formation assay

The treated H1299 and Calu-3 cells were seeded in six-well plates ($\sim 1 \times 10^3$ cells/well) and cultured for 14 d in a 37 °C incubator with 5% CO₂. Afterward, the cells were washed with phosphate-buffered saline (PBS), fixed with 4% paraformaldehyde, and stained with 1% crystal violet for 15 min. The number of cell colonies was calculated under an optical microscope (Carl Zeiss, Oberkochen, Germany) thereafter.

2.5. Terminal deoxynucleotidyl transferase (TdT)-mediated dUTP nick end labeling (TUNEL)

Apoptosis of cells was analyzed following the instruction manual of the One-step TUNEL In Situ Apoptosis Kit (Elabscience Biotechnology Co., Ltd., Wuhan, Hubei, China). In short, the cells were incubated with TdT and dTUP at 37 °C for 2 h. Nuclei were stained with 4', 6-diamidino-2-phenylindole. The labeling was observed under a fluorescence microscope (Olympus Optical Co., Ltd, Tokyo, Japan), and the TUNEL-positive rate was calculated.

2.6. Chromatin immunoprecipitation (ChIP)-qPCR

According to the instructions of the Simple ChIP™ Enzymatic ChromatinIP Kit (Cell Signaling Technologies [CST], Beverly, MA, USA), exponentially growing H1299 and Calu-3 cells ($\sim 1 \times 10^6$) were cross-linked in 4% formaldehyde for 10 min, followed by centrifugation and ultrasonication to truncate chromatin into fragments. The chromatin solution was pre-treated with 50 μL of ChIP-Grade protein G magnetic beads, followed by IP reaction with the antibodies of EP300 (1:1,000, #12281, CST), H3K27ac (1:500, GTX128944, GeneTex Inc., San Antonio, TX, USA) or IgG (1:1,000, #6990, CST) at 4 °C overnight. The antibody-chromatin complexes were collected and de-crosslinked, and the DNA was eluted and purified to examine the enrichment of SLC16A1-AS1 promoter fragments. The SLC16A1-AS1 promoter sequence used is below: F: 5'-CCCTCAGTTTCTGCCAGAGA-3', R: 5'-ACTTCCCGAGGTCACCT-GAAC-3'.

2.7. RNA immunoprecipitation (RIP)

Following the instruction manual of the Magna RIP Quad Kit (Merck), the H1299 and Calu-3 cells were lysed in the RIP lysis buffer. Later, the Protein A/G magnetic beads were incubated with anti-m6A (1:1,000, ab208577, Abcam), anti-YTHDF1 (1:50, #86463, CST), anti-YTHDF2 (1:100, +80014, CST), anti-YTHDF3 (1:100, #24206, CST) or rabbit IgG (1:200, ab109489, Abcam) at 20–25 °C for 1 h. Treated magnetic beads were incubated with 100 μL at 4 °C for 12 h. After proteinase treatment, the FOXP3 mRNA expression in the precipitation was analyzed by RT-qPCR.

2.8. Western blot (WB) analysis

Nuclear protein from cells or tissues was extracted using a BBproExtra® extraction kit (BB-3102, Best-Bio, Jiangsu, China). The protein concentration was examined by the BCA kit Solarbio Science & Technology, Beijing, China), followed by SDS-PAGE to transfer the protein onto a polyvinylidene fluoride membrane. The membranes were blocked by 8% non-fat milk and probed with antibodies against β-catenin (1:1,000, #8480, CST) or TCF3 (1:500, GTX637791, Genetex) overnight at 4 °C, followed by incubation with goat anti-rabbit IgG (1:100, GTX213110-01, GeneTex) at 23–25 °C for 2 h. The protein blots were visualized using the Novex™ ECL kit (Thermo Fisher Scientific), followed by quantification analysis using Quantity One. Lamin B1 (1:500, ab229025, Abcam) or β-actin (1:500, GTX109639, Genetex) was used as the internal reference. Uncropped WB bands were displayed in Supplementary Files.

2.9. Tumor xenograft models

Forty BALB/c nude mice (18 ± 2 g) were procured from Vital River Laboratory Animal Technology, Beijing, China) and used with the protocol approved by the Animal Ethics Committee of our hospital. H1299 cells (only one cell line was used to reduce animal usage) stably transfected with sh-NC, oe-NC, sh-EP300, oe-SLC16A1-AS1, sh-SLC16A1-AS1, or their combinations were injected into mice subcutaneously to induce xenograft tumors, and the injection volume was 5×10^6 cells per mouse. The tumor size was evaluated once every 5 d as follows: volume = (length × width²)/2. After 20 d, the animals were killed by injection of an overdose of nembital (130 mg/kg), and the xenograft tumors were collected and weighed.

2.10. Statistical analysis

Prism 8.0.2 (GraphPad, La Jolla, CA, USA) was applied for data analysis and graph generation. All data are expressed as the mean \pm standard deviation. Differences were analyzed by the Student's *t*-test, or the one- or two-way ANOVA, as appropriate. Tukey's multiple analysis was applied for post-hoc analysis. Significant difference was defined by a *p*-value less than 0.05.

3. Results

3.1. SLC16A1-AS1 is highly expressed in LC and correlated with malignance of tumor cells

Cancer tissues and adjacent tissues in three clinical LC patients were harvested for a lncRNA microarray analysis. A total of 361 differentially expressed lncRNAs were identified, among which SLC16A1-AS1 showed the most significant increase in expression in LC (Fig. 1A). SLC16A1-AS1 has been demonstrated to be highly expressed in glioblastoma and promote the malignant progression of cancer cells [12]. However, the underpinning molecular mechanisms are not fully clear. Subsequently, we confirmed by RT-qPCR that SLC16A1-AS1 expression was significantly upregulated in 56 pairs of LC tissues compared to the matched normal tissues (Fig. 1B). Similarly, increased expression of SLC16A1-AS1 was detected in the four LC cell lines (H1299, Calu-3, A549, and H460) compared to the normal BEAS-2B cells (Fig. 1C). H1299 and Calu-3 cells with the highest degree of upregulation were selected for subsequent cellular experiments. Three shRNAs targeting SLC16A1-AS1 were administered into these two cell lines, and the sh-SLC16A1-AS1#3 with the best suppressive efficacy was applied in the subsequent experiments (Fig. 1D). Importantly, SLC16A1-AS1 silencing significantly decreased the colony formation ability (Fig. 1E), migration, invasion (Fig. 1F and G), and the number of TUNEL-positive cells (apoptotic cells) (Fig. 1H) in the functional assays.

3.2. EP-300/H3K27ac axis mediates SLC16A1-AS1 promoter to induce its transcription

Interestingly, data in the UCSC browser (<https://genome.ucsc.edu/index.html>) suggests the existence of H3K27ac modifications near the promoter of SLC16A1-AS1 (Fig. 2A). Meanwhile, an enrichment of SLC16A1-AS1 was predicted near the SLC16A1-AS1 promoter as well (Fig. 2A). Since H3K27ac is an enhancer-associated histone mark that indicates active transcription, we conjectured that SLC16A1-AS1 is an enhancer-regulated gene. To investigate whether EP300 has a regulatory effect on SLC16A1-AS1 transcription, the ChIP-qPCR assay was performed, which revealed significant enrichment of EP300 near the SLC16A1-AS1 promoter (Fig. 2B). Thereafter, sh-EP300 was transfected into H1299 and Calu-3 cells, which successfully increased the EP300 expression (Fig. 2C), followed by a substantial downregulation of SLC16A1-AS1 in both cell lines (Fig. 2D). The ChIP assay further showed that the upregulation of EP300 in cells increased the enrichment of H3K27ac modifications near the SLC16A1-AS1 promoter (Fig. 2E). These findings suggest that EP-300 may activate the SLC16A1-AS1 transcription by promoting H3K27ac modifications near its promoter region.

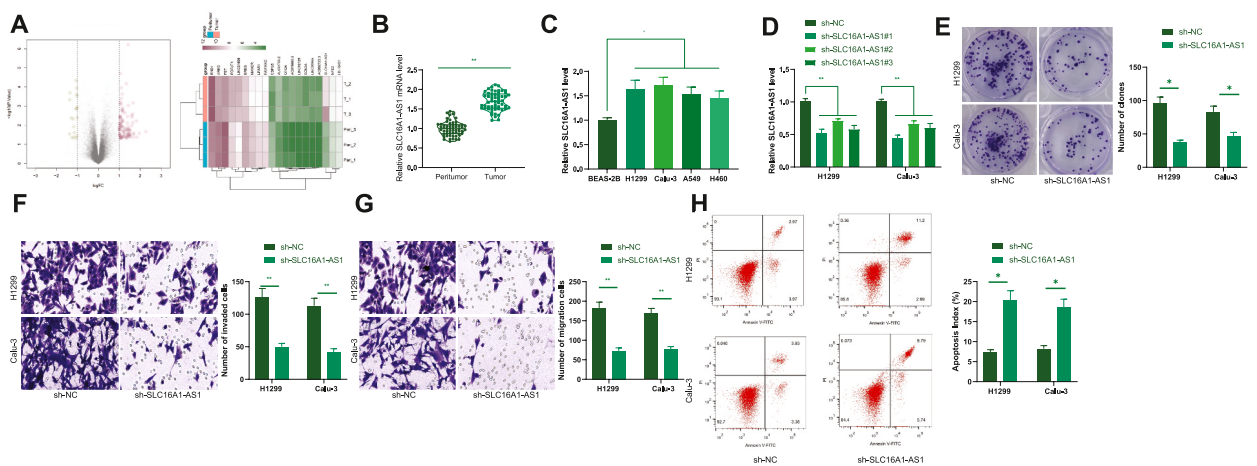


Fig. 1. SLC16A1-AS1 is highly expressed in LC and correlated with the malignance of tumor cells. A, a lncRNA microarray analysis for differentially expressed lncRNAs between three pairs of LC tumor tissues and normal tissues; B, SLC16A1-AS1 expression in 56 pairs of LC tumor tissues and normal tissues examined by RT-qPCR; C, SLC16A1-AS1 expression in LC cell lines (H1299, Calu-3, A549, and H460) and normal BEAS-2B cells examined by RT-qPCR; D, SLC16A1-AS1 expression in H1299 and Calu-3 cells after transfection of sh-SLC16A1-AS1#1–3 determined by RT-qPCR; E–F, migration and invasion of H1299 and Calu-3 cells after SLC16A1-AS1 silencing examined by Transwell assays; G, apoptosis of H1299 and Calu-3 cells after SLC16A1-AS1 silencing examined by the TUNEL assay. Three biological replicates were performed. Differences were analyzed by the paired *t*-test, or by the one-way or two-way ANOVA. **p* < 0.05.

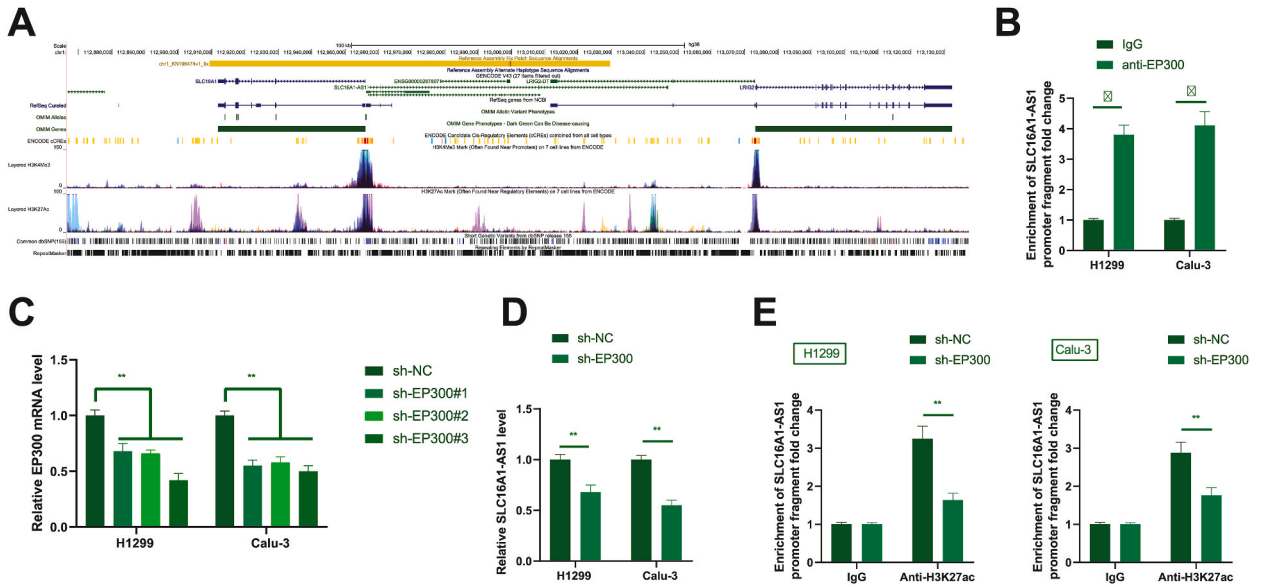


Fig. 2. EP-300/H3K27ac axis mediates the SLC16A1-AS1 promoter to induce its transcription. A, enrichments of H3K27ac modifications and EP300 near the SLC16A1-AS1 predicted using the UCSC browser; B, binding between EP300 and SLC16A1-AS1 promoter examined by the ChIP-qPCR assay; C-D, expression of EP300 mRNA (C) and SLC16A1-AS1 in H1299 and Calu-3 cells after the administration of sh-EP300 examined by RT-qPCR; E, enrichment of H3K27ac near the SLC16A1-AS1 promoter in H1299 and Calu-3 cells overexpressing EP300 examined by ChIP-qPCR. Three biological replicates were performed. Differences were analyzed by the two-way ANOVA. * $p < 0.05$.

3.3. TCF3 is highly expressed in LC and binds with SLC16A1-AS1

By analyzing the binding proteins of SLC16A1 using the RapidOmics software, we obtained TCF3 as a candidate (Fig. 3A) and focused on its interaction with SLC16A1. SLC16A1 has been demonstrated to promote the malignant development of LC cells [18]. Indeed, RT-qPCR results revealed an up-regulation pattern of TCF3 in the clinical tumor tissues as well as in the LC cell lines (H1299, Calu-3, HS 683, and T98G) compared to the normal tissues or cells (Fig. 3B and C). It was noteworthy that TCF3 showed a positive correlation with SLC16A1-AS1 in terms of their expression patterns in clinical tumor tissues (Fig. 3D). Subsequently, RIP assay verified that SLC16A1 could specifically interact with the TCF3 protein in H1299 and Calu-3 cells (Fig. 3E). Moreover, we used fluorescence co-localization experiments to verify that TCF3 had a significant binding relationship with SLC16A1-AS1 in H1299 and Calu-3 cells (Fig. 3F).

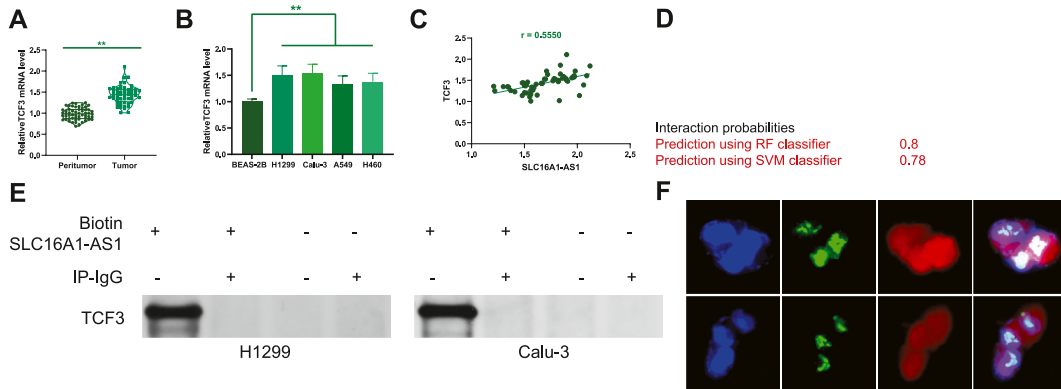


Fig. 3. TCF3 is highly expressed in LC and binds with SLC16A1-AS1. A, TCF3 as a candidate binding protein of SLC16A1 predicted by the RapidOmics analysis; B, TCF3 mRNA expression in 56 pairs of LC tumor tissues and normal tissues examined by RT-qPCR; C, SLC16A1-AS1 and TCF3 expression in LC cell lines (H1299, Calu-3, HS 683, and T98G) and normal HMC3 cells examined by RT-qPCR; D, a positive correlation between SLC16A1-AS1 and TCF3 expression in clinical LC tumor tissues; E, binding between SLC16A1 and TCF3 protein examined by RIP assay. F, Dual-labeled fluorescence staining was used for lncRNA SLC16A1-AS1 and TCF3 subcellular location. Three biological replicates were performed. Differences were analyzed by the paired *t*-test or by the one-way ANOVA. * $p < 0.05$.

3.4. The binding of SLC16A1-AS1 with TCF3 activates the Wnt/ β -catenin signaling pathway

According to the literature, TCF3 can activate the Wnt/ β -catenin pathway to promote the malignant progression of cervical cancer or LC cells. We conducted a correlation analysis of genes with a correlation coefficient greater than 0.47 related to SLC16A1-AS1 from the TCGA-LC database using the Corr R package. We performed KEGG enrichment analysis of the signal pathways where the genes associated with SLC16A1-AS1 were distributed. We observed that these genes were primarily distributed in the Wnt signaling pathway (Fig. 4A). Therefore, we hypothesize that SLC16A1-AS1 binding to TCF3 activates the Wnt/ β -catenin pathway, thus influencing LC progression. In LC cell lines with knocked-down SLC16A1-AS1, we co-overexpressed TCF3 and assessed the transfection efficiency through RT-qPCR (Fig. 4B). By performing WB, we examined β -catenin nuclear accumulation in cells subjected to different treatments (Fig. 4C and D). The results showed that knocking down SLC16A1-AS1 significantly reduced β -catenin nuclear accumulation, while co-overexpressing TCF3 led to a significant increase in β -catenin nuclear accumulation. The accumulation of β -catenin in the cell nucleus indicates the activation of the Wnt/ β -catenin pathway, suggesting that SLC16A1-AS1/TCF3 can activate the Wnt/ β -catenin pathway.

3.5. SLC16A1-AS1/TCF3 mediates Wnt/ β -catenin pathway to impact the malignant progression of LC

We treated sh-SLC16A1-AS1+oe-TCF3 LC cell lines with XAV-939. The nuclear accumulation of β -catenin in cells following different treatments was assessed using WB (Fig. 5A). Subsequently, we conducted colony formation, Transwell, and apoptosis experiments in LC cells with TCF3 overexpression and those with combined TCF3 overexpression and XAV-939 treatment to evaluate the impact of different treatments on LC cells. The results demonstrated that, compared to LC cells with suppressed SLC16A1-AS1, those with TCF3 overexpression exhibited significantly increased proliferation, migration, and invasion capabilities, and significantly decreased apoptosis. Moreover, compared to the DMSO-treated LC cells with TCF3 overexpression, XAV-939 treatment resulted in significant reductions in proliferation, migration, and invasion capabilities and a notable increase in apoptosis (Fig. 5B-E). This suggests that SLC16A1-AS1/TCF3 can mediate the Wnt/ β -catenin pathway to impact the malignant progression of LC.

In Vivo Validation of EP300 Regulating SLC16A1-AS1/TCF3-Mediated Wnt/ β -Catenin Pathway Impact on LC Malignancy.

The in vitro experimental data indicated that EP300 regulates SLC16A1-AS1/TCF3-mediated Wnt/ β -catenin pathway, influencing the malignant progression of LC. We conducted in vivo xenograft tumor experiments to validate these findings. To minimize unnecessary sacrifice of experimental animals, we selected the H1299 cell line for animal experiments. In the H1299 cell line with EP300 knockdown, we co-overexpressed SLC16A1-AS1 and assessed transfection efficiency through RT-qPCR (Fig. 6A). Stable transfections,

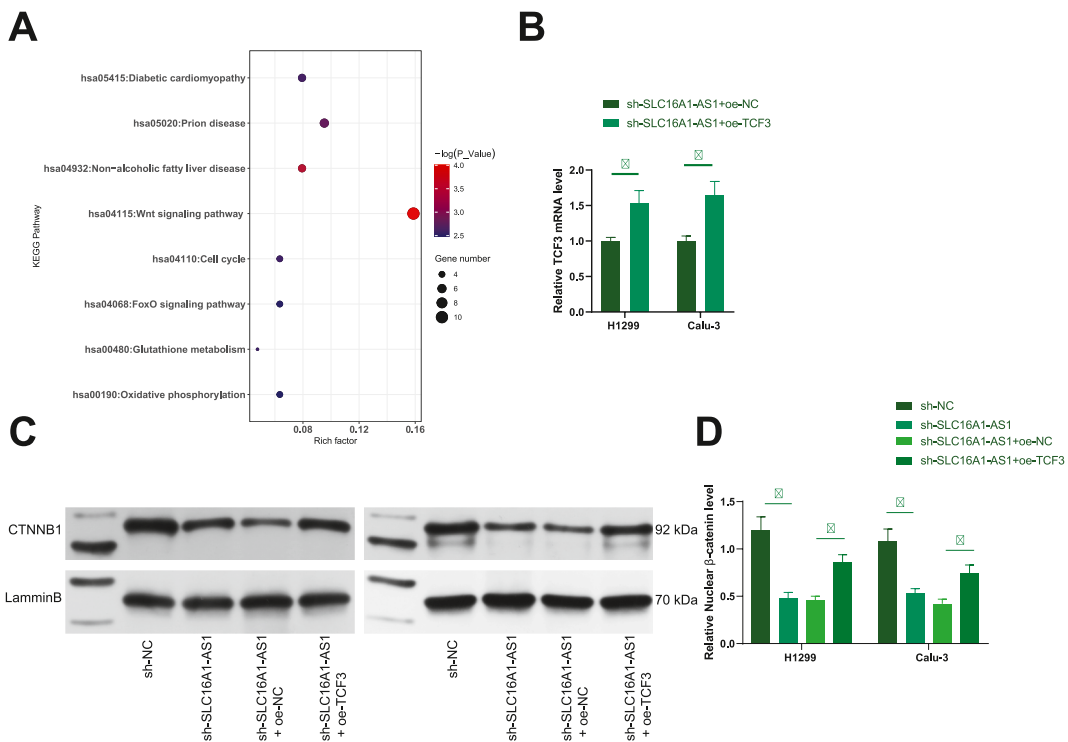


Fig. 4. SLC16A1-AS1/TCF3 Activation of the Wnt/ β -catenin Pathway A: KEGG enrichment analysis of signaling pathways associated with genes related to SLC16A1-AS1. B: RT-qPCR to assess the transfection efficiency of co-overexpressing TCF3 in LC cells with SLC16A1-AS1 knocked down. C-D: Western blot analysis to measure the nuclear accumulation of β -catenin in cells after different treatments. All cell experiments were independently repeated three times. Two-way ANOVA (B, D) was used for comparisons between multiple groups, followed by Tukey's post hoc test. *P < 0.05.

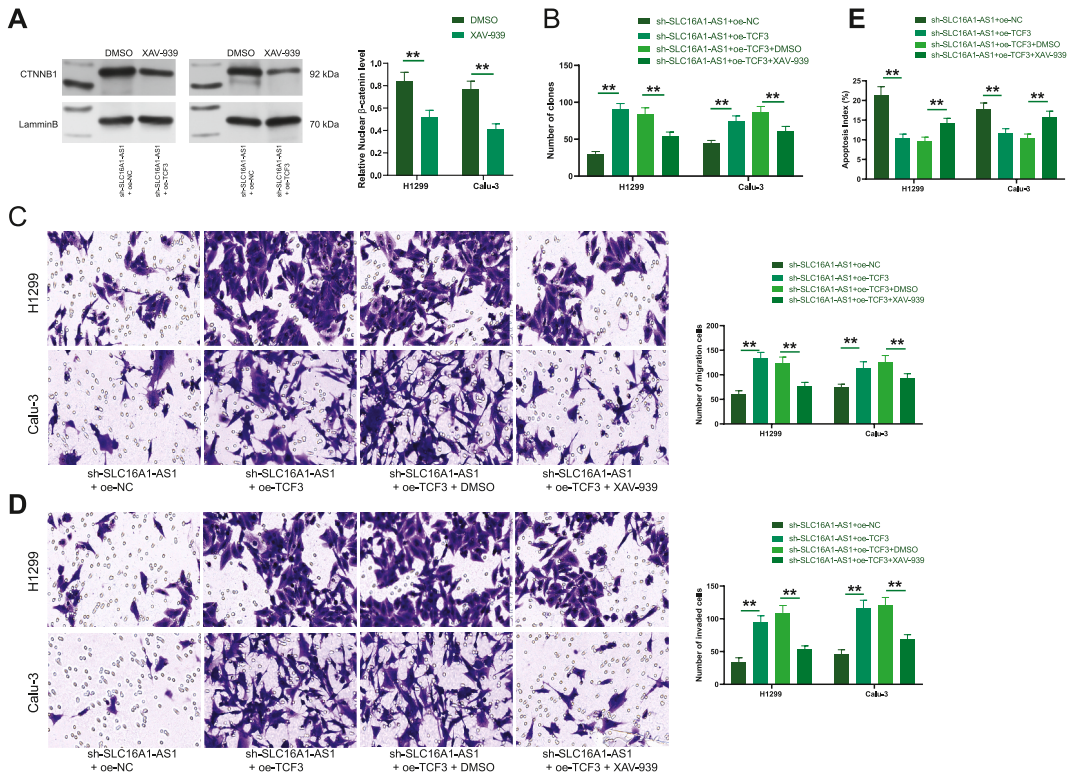


Fig. 5. SLC16A1-AS1/TCF3 Mediates the Malignant Progression of LC through the Wnt/ β -Catenin Pathway. A: Western blot (WB) showing the nuclear accumulation of β -catenin in LC cells with TCF3 overexpression and those with TCF3 overexpression treated with XAV-939. B: Colony formation assay to assess the proliferation capability of LC cells under different treatments. C–D: Transwell assay measuring the migration and invasion abilities of LC cells subjected to different treatments. E: TUNEL staining to evaluate the apoptosis rate of LC cells after various treatments. All cellular experiments were independently repeated three times. Two-way ANOVA (A–E) was employed for comparisons among multiple groups, followed by Tukey’s post hoc test. * $P < 0.05$.

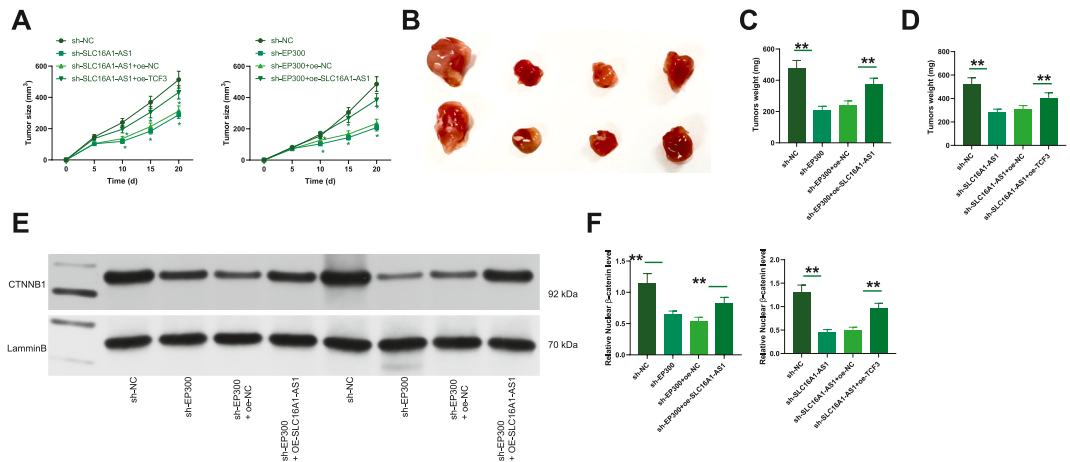


Fig. 6. In Vivo Validation of EP300 Regulating SLC16A1-AS1/TCF3-Mediated Wnt/ β -Catenin Pathway Impact on LC Malignancy. A: RT-qPCR, assessing the transfection efficiency of co-overexpressing SLC16A1-AS1 in H1299 cells with EP300 knockdown. B–D: In vivo tumor growth model, evaluating the in vivo growth capability and tumor weight of H1299 cells subjected to different treatments. E–F: Western blot (WB) measured the nuclear accumulation of β -catenin in the collected tumor masses. All cell experiments were independently repeated three times, and each group of animal experiments involved 5 mice. A Paired t -test (A) was used for comparisons between two groups, while Two-way ANOVA (B, D, F) was applied for comparisons involving multiple groups. Tukey’s post-hoc test was used. * $P < 0.05$.

including sh-NC, sh-EP300, sh-EP300+oe-NC, sh-EP300+oe-SLC16A1-AS1, sh-SLC16A1-AS1, sh-SLC16A1-AS1+oe-NC, and sh-SLC16A1-AS1+oe-TCF3 H1299 cells, were injected subcutaneously into nude mice. We monitored tumor growth rates and weighed the tumors at the end of the experiment. The results showed that after EP300 knockdown, both the tumor growth rate and final weight significantly decreased. Upon co-overexpressing SLC16A1-AS1, the tumor growth rate and final weight markedly increased. Conversely, after knocking down SLC16A1-AS1, the tumor growth rate and final weight significantly decreased. When TCF3 was co-overexpressed, the tumor growth rate and final weight showed a notable increase (Fig. 6B–D). We conducted WB analysis to assess the nuclear accumulation of β -catenin in the collected tumor masses. The results revealed that EP300 knockdown led to a significant reduction in the nuclear accumulation of β -catenin. Conversely, co-overexpressing SLC16A1-AS1 resulted in a substantial increase in β -catenin nuclear accumulation. Moreover, knocking down SLC16A1-AS1 led to a remarkable decrease in β -catenin nuclear accumulation, while co-overexpressing TCF3 caused a significant rebound in β -catenin nuclear accumulation (Fig. 6E and F).

4. Discussion

In the precision medicine era, targeted molecular therapy is the main strategy for the management of cancer patients. Hence, a deep understanding of the molecular events that underlie various biological behaviors is increasingly needed. In this work, the authors claim that the EP300-mediated H3K27ac modification leads to the transcription activation of SLC16A1-AS1, which binds to TCF3 and activates the Wnt/ β -catenin pathway to promote the malignant development of LC.

SLC16A1-AS1 attracted our concerns as the lncRNA microarray analysis suggested it exhibited the most significant aberrant high expression in LC tissues. Indeed, its high-expression pattern was then verified in tumor tissues of a cohort of 56 patients and several LC cell lines. This was in concert with the findings of previous reports [14,15]. These reports also demonstrated that SLC16A1-AS1 upregulation promoted malignant properties of LC cells. Indeed, we found that the artificial silencing of SLC16A1-AS1 inhibited proliferation, migration, and invasion, and resistance to death of H1299 (grade IV) and Calu-3 (grade III) cells. This validates the oncogenic role of SLC16A1-AS1 in LC cells as well as in non-LC cells. SLC16A1-AS1 has also been demonstrated to exhibit multiple tumorigenic features in several other human malignancies, such as oral squamous cell carcinoma [21], hepatocellular carcinoma [22], and renal cell carcinoma [23]. However, the tumor suppressive roles of SLC16A1-AS1 have also been reported in non-small LC [24] and triple-negative breast cancer [25]. The discrepancy indicates that SLC16A1-AS1 could possess distinct biological functions depending on the specific disease or tissue contexts or depending on the specific molecular mechanisms.

The existence of EP300 and H3K27ac modification peaks near the SLC16A1-AS1 promoter, as predicted by bioinformatics, aroused our concerns to investigate the interaction between EP300/H3K27ac with SLC16A1-AS1. We confirmed the binding between EP300 and the SLC16A1-AS1 promoter and found that the EP300 overexpression increased H3K27ac enrichments near the SLC16A1-AS1 promoter, thus promoting its transcription. There is always a global increase in H3K27ac while a loss in the H3K27 trimethylation (a transcriptional repressive mark) in high-grade LC, which was induced by the H3K27 M driver mutations [26,27]. As an active transcription mark, the enrichment of H3K27ac near the enhancer or promoter regions is correlated with an open chromatin state and gene activation [28]. The rule is also true for lncRNA regulation. For instance, H3K27ac modifications can activate the transcription of lncRNA KTN1-AS1 during the progression of ovarian cancer. Similarly, the high expression of FOXC2-AS1, which presented a tumor-promoting role in tongue squamous cell carcinoma, was reportedly induced by the H3K27ac modification as well [29]. Here, we opine that the aberrant activation of SLC16A1-AS1 is attributed to the EP300-mediated H3K27ac modifications.

5. Conclusion

In conclusion, the findings of this study reveal a complex regulatory network in LC involving the lncRNA SLC16A1-AS1, the epigenetic modifier EP300, the transcription factor TCF3, and the Wnt/ β -catenin signaling pathway. SLC16A1-AS1 is demonstrated to be highly expressed in LC and exerts a significant influence on the malignant progression of LC. EP300 is identified as a key mediator of histone modifications on the SLC16A1-AS1 promoter, thereby controlling its expression. Furthermore, SLC16A1-AS1 interacts specifically with TCF3, forming a complex that activates the Wnt/ β -catenin pathway. Importantly, EP300 emerges as a critical regulator in modulating the impact of the SLC16A1-AS1/TCF3-mediated Wnt/ β -catenin signaling on LC progression. These findings provide valuable insights into the molecular mechanisms underlying LC pathogenesis and suggest potential therapeutic targets for the management of this disease. However, this study is confined to some limitations. First, the clinical implications of SLC16A1-AS1/TCF3 have not validated. Second, the research on the downstream pathway is not sufficient. More investigation is required to validate the clinical implications of SLC16A1-AS1/TCF3 and downstream pathways in LC to develop therapeutic targets for early effective intervention.

Data availability

Data will be made available on request.

Ethics approval and consent to participate

The experimental protocol was established, according to the ethical guidelines of the Helsinki Declaration and was approved by the Human Ethics Committee of The First People's Hospital of Yancheng City (approval 2018-K003). Written informed consent was obtained from individual or guardian participants.

All experimental designs and protocols involving animals were approved by the Animal Ethics Committee of Jiangsu Medical

Vocational and Technical College (approval XMU 2022-861) and complied with the recommendations of the academy's animal research guidelines.

CRedit authorship contribution statement

Yunhao Sun: Formal analysis, Data curation, Conceptualization. **Jian Sun:** Software, Formal analysis, Conceptualization. **Kaijun Ying:** Software, Resources, Methodology. **Jinjin Chen:** Writing – original draft, Visualization, Validation, Data curation. **Tingting Chen:** Writing – original draft. **Leilei Tao:** Resources. **Weigang Bian:** Resources. **Limin Qiu:** Writing – review & editing, Validation, Supervision, Conceptualization.

Declaration of competing interest

The authors declare that they have no known competing financial interests or personal relationships that could have appeared to influence the work reported in this paper.

Appendix A. Supplementary data

Supplementary data to this article can be found online at <https://doi.org/10.1016/j.heliyon.2024.e27727>.

References

- [1] H. Sung, J. Ferlay, R.L. Siegel, et al., Global cancer statistics 2020: globocan estimates of incidence and mortality worldwide for 36 cancers in 185 countries, *CA: a cancer journal for clinicians* 71 (3) (2021) 209–249, <https://doi.org/10.3322/caac.21660>.
- [2] S. Thangudu, C. Yu, C. Lee, M. Liao, C. Su, Magnetic, biocompatible fe₃O₄ nanoparticles for t₂-weighted magnetic resonance imaging of in vivo lung tumors, *J. Nanobiotechnol.* 20 (1) (2022) 157, <https://doi.org/10.1186/s12951-022-01355-3>.
- [3] J. Li, L. Zhu, H.F. Kwok, Nanotechnology-based approaches overcome lung cancer drug resistance through diagnosis and treatment., *Drug Resist. Updates : reviews and commentaries in antimicrobial and anticancer chemotherapy* 66(2023) 100904, <https://doi.org/10.1016/j.drug.2022.100904>.
- [4] W. Chen, R. Zheng, P.D. Baade, et al., Cancer statistics in China, 2015., *CA, a cancer journal for clinicians* 66 (2) (2016) 115–132, <https://doi.org/10.3322/caac.21338>.
- [5] Y. Mao, D. Yang, J. He, M.J. Krasna, Epidemiology of lung cancer, *Surg. Oncol. Clin.* 25 (3) (2016) 439–445, <https://doi.org/10.1016/j.soc.2016.02.001>.
- [6] S. Couraud, G. Zalcman, B. Milleron, F. Morin, P. Souquet, Lung cancer in never smokers—a review, *Eur. J. Cancer* 48 (9) (2012) 1299–1311, <https://doi.org/10.1016/j.ejca.2012.03.007>.
- [7] S. Jonna, D.S. Subramaniam, Molecular diagnostics and targeted therapies in non-small cell lung cancer (nscl): an update, *Discov. Med.* 27 (148) (2019) 167–170.
- [8] N. Wang, C. Yu, T. Xu, et al., Self-assembly of dna nanostructure containing cell-specific aptamer as a precise drug delivery system for cancer therapy in non-small cell lung cancer, *J. Nanobiotechnol.* 20 (1) (2022) 486, <https://doi.org/10.1186/s12951-022-01701-5>.
- [9] S.R. Broderick, Adjuvant and neoadjuvant immunotherapy in non-small cell lung cancer, *Thorac. Surg. Clin.* 30 (2) (2020) 215–220, <https://doi.org/10.1016/j.thorsurg.2020.01.001>.
- [10] N. Duma, R. Santana-Davila, J.R. Molina, Non-small cell lung cancer: epidemiology, screening, diagnosis, and treatment, *Mayo Clin. Proc.* 94 (8) (2019) 1623–1640, <https://doi.org/10.1016/j.mayocp.2019.01.013>.
- [11] Q.W. Chen, Q.Q. Cai, Y. Yang, et al., Lncrna bc promotes lung adenocarcinoma progression by modulating impad1 alternative splicing, *Clin. Transl. Med.* 13 (1) (2023) e1129, <https://doi.org/10.1002/ctm2.1129>.
- [12] X. Wang, M. Sun, Z. Gao, et al., N-nitrosamines-mediated downregulation of lncrna-ucal induces carcinogenesis of esophageal squamous by regulating the alternative splicing of fgfr2., *The Science of the total environment* 855(2023) 158918, <https://doi.org/10.1016/j.scitotenv.2022.158918>.
- [13] Z. Yu, H. Tang, S. Chen, et al., Exosomal loc85009 inhibits docetaxel resistance in lung adenocarcinoma through regulating atg5-induced autophagy., *Drug Resist. Updates : reviews and commentaries in antimicrobial and anticancer chemotherapy* 67(2023) 100915, <https://doi.org/10.1016/j.drug.2022.100915>.
- [14] Y. Long, H. Li, Z. Jin, X. Zhang, Lncrna slc16a1-as1 is upregulated in glioblastoma and promotes cancer cell proliferation by regulating mir-149 methylation., *Cancer Manag. Res.* 13(2021) 1215–1223, <https://doi.org/10.2147/CMAR.S264613>.
- [15] Z. Jin, H. Li, Y. Long, R. Liu, X. Ni, Microrna-1269 is downregulated in glioblastoma and its maturation is regulated by long non-coding rna slc16a1 antisense rna 1., *Bioengineered* 13 (5) (2022) 12749–12759, <https://doi.org/10.1080/21655979.2022.2070581>.
- [16] R. Raisner, R. Bainer, P.M. Haverty, K.L. Benedetti, K.E. Gascoigne, Super-enhancer acquisition drives oncogene expression in triple negative breast cancer, *PLoS One* 15 (6) (2020) e235343, <https://doi.org/10.1371/journal.pone.0235343>.
- [17] E.T. Manning, T. Ikehara, T. Ito, J.T. Kadonaga, W.L. Kraus, P300 forms a stable, template-committed complex with chromatin: role for the bromodomain, *Mol. Cell Biol.* 21 (12) (2001) 3876–3887.
- [18] A.D. Durbin, T. Wang, V.K. Wimalasena, et al., Ep300 selectively controls the enhancer landscape of mycn-amplified neuroblastoma, *Cancer Discov.* 12 (3) (2022) 730–751, <https://doi.org/10.1158/2159-8290.CD-21-0385>.
- [19] L. Huang, L. Li, B. Cheng, T. Xing, Slc38a6, regulated by ep300-mediated modifications of h3k27ac, promotes cell proliferation, glutamine metabolism and mitochondrial respiration in hepatocellular carcinoma, *Carcinogenesis* 43 (9) (2022) 885–894, <https://doi.org/10.1093/carcin/bgac061>.
- [20] D.E. de Almeida Nagata, E.Y. Chiang, S. Jhunjhunwala, et al., Regulation of tumor-associated myeloid cell activity by cbp/ep300 bromodomain modulation of h3k27 acetylation, *Cell Rep.* 27 (1) (2019) 269–281, <https://doi.org/10.1016/j.celrep.2019.03.008>.
- [21] H. Feng, X. Zhang, W. Lai, J. Wang, Long non-coding rna slc16a1-as1: its multiple tumorigenesis features and regulatory role in cell cycle in oral squamous cell carcinoma, *Cell Cycle* 19 (13) (2020) 1641–1653, <https://doi.org/10.1080/15384101.2020.1762048>.
- [22] J. Tian, D. Hu, Lncrna slc16a1-as1 is upregulated in hepatocellular carcinoma and predicts poor survival, *Clin. Res. Hepatol. Gastroenterol.* 45 (2) (2021) 101490, <https://doi.org/10.1016/j.clinre.2020.07.001>.
- [23] Y.Z. Li, H.C. Zhu, Y. Du, H.C. Zhao, L. Wang, Silencing lncrna slc16a1-as1 induced ferroptosis in renal cell carcinoma through mir-143-3p/slc7a11 signaling., *Technol. Cancer Res. Treat.* 21(2022) 2081147605, <https://doi.org/10.1177/15330338221077803>.
- [24] H.Y. Liu, S.R. Lu, Z.H. Guo, et al., Lncrna slc16a1-as1 as a novel prognostic biomarker in non-small cell lung cancer, *J. Invest. Med. : the official publication of the American Federation for Clinical Research* 68 (1) (2020) 52–59, <https://doi.org/10.1136/jim-2019-001080>.
- [25] B. Jiang, Q. Liu, J. Gai, J. Guan, Q. Li, Lncrna slc16a1-as1 regulates the mir-182/pdcd4 axis and inhibits the triple-negative breast cancer cell cycle, *Immunopharmacol. Immunotoxicol.* 44 (4) (2022) 534–540, <https://doi.org/10.1080/08923973.2022.2056482>.

- [26] B. Krug, N. De Jay, A.S. Harutyunyan, et al., Pervasive h3k27 acetylation leads to erv expression and a therapeutic vulnerability in h3k27m gliomas, *Cancer Cell* 35 (5) (2019) 782–797, <https://doi.org/10.1016/j.ccell.2019.04.004>.
- [27] L. Xu, Y. Chen, Y. Huang, et al., Topography of transcriptionally active chromatin in glioblastoma, *Sci. Adv.* 7 (18) (2021), <https://doi.org/10.1126/sciadv.abd4676>.
- [28] R. Ye, C. Cao, Y. Xue, Enhancer rna: biogenesis, function, and regulation, *Essays Biochem.* 64 (6) (2020) 883–894, <https://doi.org/10.1042/EBC20200014>.
- [29] C. Chen, Q. Chen, J. Wu, H. Zou, H3k27ac-induced foxc2-as1 accelerates tongue squamous cell carcinoma by upregulating e2f3, *J. Oral Pathol. Med. : official publication of the International Association of Oral Pathologists and the American Academy of Oral Pathology* 50 (10) (2021) 1018–1030, <https://doi.org/10.1111/jop.13232>.